© 2017. Published by The Company of Biologists Ltd | Journal of Experimental Biology (2017) 220, 3162-3171 doi:10.1242/jeb.159475

RESEARCH ARTICLE

Passive regeneration of glutathione: glutathione reductase regulation in the freeze-tolerant North American wood frog, *Rana sylvatica*

Neal J. Dawson[1,*] and Kenneth B. Storey[2]

ABSTRACT

Wood frogs inhabit a broad range across North America, extending from the southern tip of the Appalachian Mountains to the northern boreal forest. Remarkably, they can survive the winter in a frozen state, where as much as 70% of their body water is converted into ice. Whilst in the frozen state, their hearts cease to pump blood, causing their cells to experience ischemia, which can dramatically increase the production of reactive oxygen species within the cell. To overcome this, wood frogs have elevated levels of glutathione, a primary antioxidant. We examined the regulation of glutathione reductase, the enzyme involved in recycling glutathione, in both the frozen and unfrozen (control) state. Glutathione reductase activity from both the control and frozen state showed a dramatic reduction in substrate specificity (K_m) for oxidized glutathione (50%) when measured in the presence of glucose (300 mmol l^{-1}) and a increase (157%) when measured in the presence of levels of urea (75 mmol l^{-1}) encountered in the frozen state. However, when we tested the synergistic effect of urea and glucose simultaneously, we observed a substantial reduction in the K_m for oxidized glutathione (43%) to a value similar to that with glucose alone. In fact, we found no observable differences in the kinetic and structural properties of glutathione reductase between the two states. Therefore, a significant increase in the affinity for oxidized glutathione in the presence of endogenous levels of glucose suggests that increased glutathione recycling may occur as a result of passive regulation of glutathione reductase by rising levels of glucose during freezing.

KEY WORDS: Antioxidants, Enzyme kinetics, Freezing, Metabolic rate depression, Phosphorylation

INTRODUCTION

The North American wood frog, *Rana sylvatica* (syn: *Lithobates sylvaticus*), is able to overwinter in a remarkable fashion; it freezes solid where up to 70% of its total body water is converted into extracellular ice (Rubinsky et al., 1990). However, the wood frog limits the amount of dehydration and quells subsequent damage to cell shape and membrane integrity by accumulating and distributing low molecular weight carbohydrate cryoprotectants, primarily glucose, to reduce osmotic pressure (Storey and Storey, 1984; Costanzo et al., 1993; Costanzo and Lee, 1993). The production of glucose, among other cryoprotectants, is achieved rapidly during the initial stages of freezing (first few hours) before blood circulation is halted, and can rise to as high as 250 mmol l^{-1} naturally, while further studies have shown that wood frogs can sustain levels of as much as 650 mmol l^{-1} glucose (Storey and Storey, 1984; Costanzo et al., 1993). In addition to glucose, urea is thought to act as an important cryoprotectant and possible driving force behind metabolic rate depression for *R. sylvatica* (Muir et al., 2008). *Rana sylvatica* has been reported to be able to accumulate as much as 80 mmol l^{-1} urea in skeletal muscles (Muir et al., 2008). The accumulation of these cryoprotectants can help offset osmotic stress; however, many complications still remain, and little is known of their effects on the activity of important cellular processes.

Overwintering in the frozen state exposes the wood frog to extreme hardships including ischemic conditions in the cells as a result of the complete cessation of cardiac function, resulting in a halt in blood flow (Rubinsky et al., 1990; Storey, 1990). Wood frogs employ a host of defenses against ischemic insult imposed by freezing, including dramatically depressing their metabolic rate to balance energy demands with limited energy production, sustaining high levels of antioxidants, and increasing the total antioxidant capacity by augmenting the activity or function of key enzymes including superoxide dismutase (SOD), glutathione peroxidase (GPx), glutathione *S*-transferase (GST) and catalase (Joanisse and Storey, 1996; Cowan and Storey, 2001; Dawson et al., 2015; Dawson and Storey, 2016).

As the frog freezes, the overall reducing environment of the cells increases as oxygen is depleted as the final electron acceptor during aerobic metabolism (Joanisse and Storey, 1996). Because oxygen is exhausted in the frozen state, the electron transport chain is fully reduced, essentially priming the cell for reactive oxygen species (ROS) production. In order to combat the increasingly reduced state of the cell, as well as the burst production of free radicals during reperfusion, *R. sylvatica* has markedly higher levels of reduced glutathione (GSH; 219±17 nmol g^{-1} wet mass) in skeletal muscle compared with its non-freezing cousin *Rana pipiens* (19.9±1.8 nmol g^{-1} wet mass) (Joanisse and Storey, 1996). The levels of GSH in the muscle of *R. sylvatica* were also observed to increase significantly during freezing in *R. sylvatica*, to 308±21 nmol g^{-1} wet mass (Joanisse and Storey, 1996). An increase in total GSH levels could counteract an increase in the production of ROS during freeze-induced ischemia or reperfusion during thawing.

GSH is the most abundant non-protein thiol in cells and plays a primary role as an antioxidant in mammalian cells (Meister, 1995). The role of GSH as an antioxidant can be divided into two main functions: direct interaction with ROS or as an electron donor to antioxidant enzymes such as GPx, GST and glutaredoxin (GRX) (Meyer et al., 2009). Glutathione exists in two forms, the reduced form (GSH) or the oxidized form (GSSG), the latter arising from the

[1]Department of Biology, McMaster University, 1280 Main Street West, Hamilton, ON, Canada L8S 4K1. [2]Department of Biology and Institute of Biochemistry, Carleton University, Ottawa, ON, Canada K1S 5B6.

*Author for correspondence (neal.dawson@gmail.com)

N.J.D., 0000-0001-5389-8692; K.B.S., 0000-0002-7363-1853

Received 14 March 2017; Accepted 25 June 2017

Journal of Experimental Biology

Journal of Experimental Biology (2017) 220, 3162-3171 doi:10.1242/jeb.159475

disulfide linkage of two GSH molecules. Glutathione reductase (GR; E.C. 1.8.1.7; also known as glutathione disulfide reductase) is a secondary antioxidant enzyme involved in the reduction of glutathione disulfide (GSSG) into two glutathione molecules (GSH). Specifically, GR catalyzes the following reaction:

$$GSSG + NADPH + H^+ \rightarrow 2\,GSH + NADP^+.$$

Primary antioxidant enzymes use GSH to detoxify ROS species and GR is the main enzyme tasked with actively recycling oxidized GSSG back to GSH. In vertebrates, GR typically has only one gene, *gsr*, as in *Xenopus* and humans. GR from *Xenopus tropicalis* or *Xenopus laevis* has a molecular mass of 51.8 kDa as reported in the UniProtKB database (B1WBJ3_XENTR, Q58E89_XENLA; Klein et al., 2002). The active site of GR has two key tyrosine residues that stabilize NADPH and GSSG during catalysis (Krauth-Siegel et al., 1998).

GR plays a major role in maintaining the GSH/GSSG ratio in the cell. Maintenance of this ratio is crucial, as GSH deficiencies cause severe oxidative shock to cells and can lead to apoptotic or necrotic cell death (Galluzzi et al., 2007; Circu and Aw, 2008; Franco and Cidlowski, 2009). In fact, keeping GSH levels high has been shown to be beneficial in apoptosis-resistant models (Armstrong et al., 2002; Friesen et al., 2004). Although GSH is found in high amounts (millimolar levels) in the cytoplasm, GSH also exists in many organelles in the cell, including the mitochondria, peroxisomes, nuclear matrix and the endoplasmic reticulum (Forman et al., 2009). Mitochondria are incapable of *de novo* synthesis of GSH, which suggests that the importance of GSH is amplified in the mitochondria, the organelle with perhaps the highest continuous generation of ROS in association with running the electron transport system (Galluzzi et al., 2007; Circu and Aw, 2008). This emphasizes the crucial role of mitochondrial GR in recycling GSH from GSSG. It has been proposed that both GR and GSH must be actively transported into the mitochondrial matrix (Franco and Cidlowski, 2009). The roles of mitochondrial and cytosolic levels of GSH have been explored independently, and oxidative stress has been linked to both in a similar fashion, suggesting that their roles may in fact not be independent of one another (Garcia-Ruiz and Fernandez-Checa, 2006; Lash, 2006).

Cytosolic and mitochondrial GSH pools seem to be critically important to counteract the production of ROS during reoxygenation of cells, and reactivation of the electron transport chain in the mitochondria following ischemic stress (Muyderman et al., 2007). This may cause certain sites of burst ROS production, such as the mitochondria, to overwhelm the GSH pools at the site of insult during or preceding ischemic stress. One of the main ROS produced in the mitochondria is superoxide (O_2^-). O_2^- cannot cross the mitochondrial membrane, and either reacts with GSH or other antioxidants or is converted into H_2O_2 by manganese superoxide dismutase (MnSOD). GR plays a pivotal role in maintaining the redox state of the cell, specifically the GSSG/GSH ratio, and maintenance of the mitochondrial ratio of GSSG/GSH has also been linked to the suppression of apoptosis (Marchetti et al., 1997; Muyderman et al., 2007).

GR has been widely studied and characterized from humans and traditional animal models; however, less is known about its role in disease states or in aiding survival in the freezing frog. This study presents the first investigation of the potential method of regulation of GR in the leg muscle of *R. sylvatica*, comparing control and frozen states, and provides evidence of possible regulation by rising glucose levels.

MATERIALS AND METHODS

Chemicals

All chemicals were from BioShop (Burlington, ON, Canada) with a few exceptions: oxidized glutathione (GSSG) was from Sigma (St Louis, MO, USA), Cibacron Blue column was from Affiland (Ans, Belgium), hydroxyapatite Bio-Gel® HTP Gel column was from Bio-Rad (Hercules, CA, USA) and potassium phosphate, monobasic was from J. T. Baker Chemical Company (London, UK).

Animals

Male wood frogs, *Rana sylvatica* LeConte 1825, were collected from the Ottawa area in the spring and, upon capture, were washed in a tetracycline bath. Sixteen frogs were then placed in containers containing damp sphagnum moss and held at 5°C for 1 week. The frogs were separated into two different groups. Eight control frogs were sampled directly from the 5°C group. Eight frozen frogs were placed in closed boxes with damp paper towel lining the bottom and placed in an incubator set at −3°C. The frogs were cooled over a 45 min period to allow the body temperature of the frogs to fall to below −0.5°C. Ice nucleation was achieved through skin contact with ice crystals formed on the wet paper towel. The frozen group of frogs was kept under these conditions for 24 h. Both control and frozen frogs were killed by pithing and tissues were quickly excised and frozen in liquid N_2. All tissue samples were stored at −80°C until later use. The Carleton University Animal Care Committee, in accordance with the Canadian Council on Animal Care guidelines, approved all animal handling protocols used during this study.

Preparation of muscle tissue lysates for protein purification

For protein purification, samples of frozen muscle tissue were homogenized 1:5 w:v in ice-cold homogenizing buffer A [50 mmol l^{-1} potassium phosphate (KPi) buffer, pH 7.2, containing 30 mmol l^{-1} β-glycerophosphate, 1 mmol l^{-1} EGTA, 1 mmol l^{-1} EDTA, 15 mmol l^{-1} β-mercaptoethanol, 10% glycerol and 1 mmol l^{-1} phenylmethylsulfonyl fluoride (PMSF)]. Homogenates were then centrifuged at 13,500 ***g*** at 4°C and the supernatant was collected for use in protein purification.

Purification of GR

A 5 cm column of Sephadex G-50 in a syringe barrel was equilibrated in buffer A and centrifuged at 500 ***g*** in a bench-top centrifuge for 2 min to remove excess buffer. An aliquot of 2 ml of frog muscle tissue supernatant was applied to the column and centrifuged again. The resulting eluant was collected. A hydroxyapatite column (1.5 cm×2 cm) was then washed with 20 ml of buffer A to equilibrate the column. The eluant collected from the Sephadex G-50 column was applied to the hydroxyapatite column and washed with 20 ml buffer A to remove unbound proteins. GR was eluted from the hydroxyapatite column with a linear gradient of 0–3.5 mol l^{-1} KCl in buffer A. The four fractions (with highest activity) of 900 µl were collected and 10 µl from each fraction was assayed to detect GR activity (see 'Kinetic assays' section below for methodology). The fractions of peak GR activity were pooled and diluted 10-fold with buffer A. The diluted fractions were applied to a Cibacron Blue column (1.5 cm×10 cm) pre-washed with 50 ml of buffer A. The column was washed with a further 50 ml of buffer A to remove unbound protein and then bound protein was eluted with a linear gradient of 0–2 mol l^{-1} KCl in homogenization buffer A. The top four fractions (with highest activity) of 450 µl were collected and 20 µl from each fraction was assayed to detect GR activity. To assess enzyme purity, aliquots of GR from different stages of the purification procedure were

Journal of Experimental Biology (2017) 220, 3162-3171 doi:10.1242/jeb.159475

combined 2:1 with SDS loading buffer (100 mmol l^{-1} Tris buffer, pH 6.8, 4% w/v SDS, 20% v/v glycerol, 0.2% w/v Bromophenol Blue, 10% v/v 2-mercaptoethanol), boiled for 5 min, and then 20 µl samples were used for SDS-PAGE as described below.

Kinetic assays

GR was assayed using a modified version of the method of Di Ilio et al. (1983). Assay conditions were: 50 mmol l^{-1} KPi buffer (pH 7.2), 2 mmol l^{-1} GSSG, 0.25 mmol l^{-1} NADPH and 10 µl tissue extract. One unit of enzyme activity is the amount that oxidizes 1 µmol of NADPH per minute at 25°C. The amount of NADPH was measured at 340 nm in a Thermo Labsystems Multiskan spectrophotometer (Thermo Scientific, Waltham, MA, USA). Enzyme affinity for GSSG was determined in the presence versus absence of 75 mmol l^{-1} urea or 300 mmol l^{-1} glucose. Activation of GR by adenosine triphosphate (ATP), adenosine diphosphate (ADP), adenosine monophosphate (AMP), Mg^{2+}, Mn^{2+}, K^{+}, Ca^{2+} or Zn^{2+} was also tested. Data were analyzed using the Kinetics v.3.5.1 program (Brooks, 1992).

Gel electrophoresis

GR was purified as described above. Protein separation was achieved by running 20 µl of GR samples on 10% SDS-PAGE gels. Sample aliquots were loaded onto polyacrylamide gels together with PageRuler® pre-stained size (10–180 kDa) standards (Thermo Scientific, cat no. 26616) and separated using a discontinuous buffer system. Electrophoresis was carried out at 180 V for 65 min using the Bio-Rad Mini-Protean 3 system with 1× Tris-glycine running buffer (0.05 mol l^{-1} Tris, 0.5 mol l^{-1} glycine, 0.05% w/v SDS). Protein banding was visualized with Coomassie Blue.

Pro-Q Diamond phosphoprotein staining

Muscle GR from control and frozen frogs was purified as described above. The top four fractions based on activity were pooled, and protein levels in the pooled fractions were quantified using the Coomassie Blue dye-binding method. Aliquots of the pooled fractions were then mixed 1:1 v:v with SDS loading buffer (100 mmol l^{-1} Tris buffer, pH 6.8, 4% w/v SDS, 20% v/v glycerol, 0.2% w/v Bromophenol Blue, 10% v/v 2-mercapotethanol), subsequently boiled for 5 min and stored at −20°C until used.

Equal volumes of each sample were loaded on a 10% SDS-PAGE gel. The gel was run at 180 V for 55 min in running buffer (0.5 mol l^{-1} Tris, 5 mol l^{-1} glycine, 0.5% w/v SDS). The gel was removed and washed in fixing solution (50% v/v methanol, 10% v/v acetic acid) twice for 10 min, then left in fixing solution overnight at 4°C followed by 3 washes with ddH_2O for 10 min. The gel was then stained with Pro-Q Diamond phosphoprotein stain (Invitrogen, Eugene, OR, USA) for 90 min and washed 3 times with ddH_2O for 10 min. The gel was covered during staining (and for the remainder of the protocol) with aluminium foil to prevent the photosensitive stain from interacting with light. To minimize non-specific background, the gel was washed in Pro-Q Diamond destaining solution (20% v/v acetonitrile, 50 mmol l^{-1} sodium acetate, pH 4) for 45 min, and then washed 3 times in ddH_2O for 10 min. The bands on the gel were visualized using the ChemiGenius Bioimaging System (Syngene, Frederick, MD, USA) to assess the relative intensities of the fluorescent bands. The fluorescence of the bands was quantified using the accompanying GeneTools software (Syngene).

In vitro incubation to stimulate protein kinases

Frog muscle tissue extracts, prepared as described above, were filtered through a Sephadex G-50 spun column equilibrated in incubation buffer (50 mmol l^{-1} KPi, 10% v:v glycerol, 30 mmol l^{-1} β-mercaptoethanol, pH 7.2). Aliquots of the filtered supernatants were incubated for 12 h at 4°C with specific inhibitors and stimulators of protein kinases, as described in Macdonald and Storey (1999). Each aliquot was mixed 2:1 v:v with the appropriate solutions to stimulate protein kinases. Each solution was prepared in incubation buffer and the following incubation conditions were used: (i) STOP conditions: 2.5 mmol l^{-1} EGTA, 2.5 mmol l^{-1} EDTA and 30 mmol l^{-1} β-glycerophosphate (designed to inhibit both kinases and phosphatases); (ii) stimulation of endogenous kinases: 5 mmol l^{-1} MgATP, 30 mmol l^{-1} β-glycerophosphate,1 mmol l^{-1} cAMP (to stimulate protein kinase A, PKA), 1 mmol l^{-1} cGMP (for protein kinase G, PKG), 1.3 mmol l^{-1} $CaCl_2$+7 µg ml^{-1} phorbol 12-myristate 13-acetate (PMA; for protein kinase C, PKC), 1 mmol l^{-1} AMP (for AMP kinase, AMPK) and 1 U of calf intestine calmodulin +1.3 mmol l^{-1} $CaCl_2$ (for Ca^{2+}/calmodulin-dependent protein kinase, CaMK).

GR was then purified and samples were analyzed using Pro-Q diamond phosphoprotein stain as described above. Fig. 1 shows the elution profile for control and frozen preparations from a $DEAE^{+}$ column. There was no significant difference in the elution profiles.

Western blotting analysis of post-translational modifications of GR

Electrophoresis was carried out as previously described. Proteins on the gel were then electroblotted onto polyvinylidene difluoride (PVDF) membrane (Millipore, Bedford, MA, USA) using a Bio-Rad mini Trans-Blot cell. The transfer was carried out at 160 mA for 1.5 h. Following the transfer, membranes were washed in TBST (10 mmol l^{-1} Tris, pH 7.5, 150 mmol l^{-1} NaCl, 0.05% v/v Tween-20) for 3×5 min. The membranes were blocked using 0.1% polyvinyl alcohol in TBST for 30 min then probed for 3 h at room temperature (RT) with the following primary antibodies (all from Invitrogen, Carlsbad, CA, USA) diluted 1:500 v:v in TBST: (1) rabbit anti-phosphoserine (cat. no. 618100), (2) rabbit anti-phosphothreonine (cat. no. 718200) or (3) rabbit anti-phosphotyrosine (cat. no. 615800). The membranes were washed 3×5 min with TBST at RT and probed with goat anti-rabbit–peroxidase secondary antibody for 20 min. Membranes were again washed 3×5 min in TBST at RT. Blots were developed with

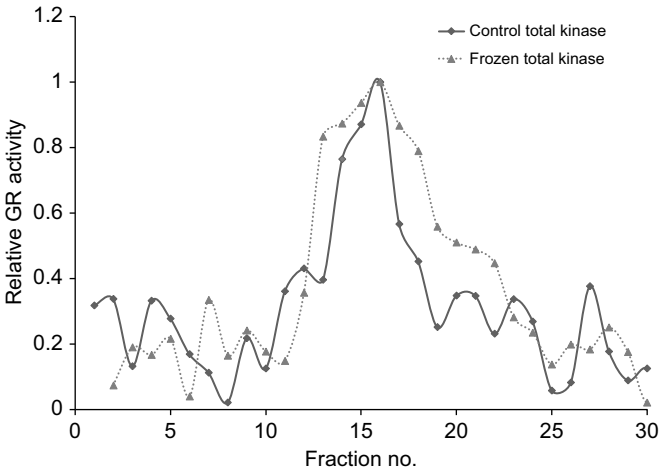

Fig. 1. $DEAE^{+}$ elution profiles for purified glutathione reductase (GR) from control and 24 h frozen *Rana sylvatica* muscle after incubation to stimulate protein kinases.

Journal of Experimental Biology (2017) 220, 3162-3171 doi:10.1242/jeb.159475

enhanced chemiluminescence reagents. Images were captured using a ChemiGenius Bio-Imaging system with GeneSnap software and densitometry analysis performed using GeneTools software (Syngene). The intensity of the immunoreactive bands was standardized against corresponding Coomassie Blue stained bands. The intensity of the standardized immunoreactive bands of GR from control muscle was set to a reference value of 1, whereas the intensity of standardized immunoreactive bands from frozen muscle was expressed as a fold change.

Arrhenius plots

Maximal GR activity was determined at 5°C increments from 5°C to 45°C. The reaction temperature was altered by placing the Thermo Labsystems Multiskan spectrophotometer into a VWR International BOD 2020 Incubator (Sheldon Manufacturing Inc., Cornelius, OR, USA) set to the desired temperature. Microplates filled with assay mixture (but without enzyme) were equilibrated in the same incubator for several minutes until the desired temperature was reached (as measured by a telethermometer). Plates were then placed into the spectrophotometer and reactions were initiated by the addition of enzyme. Arrhenius plots were constructed from these experiments and the activation energy (E_a) was calculated.

Determination of protein stability

Differential scanning fluorimetry is a high-throughput method that monitors the thermal unfolding of proteins in the presence of a fluorescent dye (Niesen et al., 2007). Purified control and 24 h frozen GR was aliquoted to a concentration of approximately 0.1 µg µl^{-1} per well into the wells of a 96-well, thin-walled PCR plate along with the dye SYPRO Orange (40× final concentration, Invitrogen) to a total volume of 20 µl. PCR plates were then sealed with sealing tape and placed into a Bio-Rad iCycler5 PCR instrument. SYPRO Orange fluorescence was monitored as described by Biggar et al. (2012). Briefly, SYPRO Orange was excited via the transmission of light through the FAM filter (485±30 nm), with the subsequent emission of light through the ROX filter (625±30 nm). Measurements were taken every 30 s at 1°C increments from 25 to 97°C. Subsequent analysis of the fluorescence data using OriginPro 8.5 and the Boltzmann distribution curve yielded the midpoint temperature of the protein unfolding transition, known as the protein melting temperature (T_m), for control and frozen frog muscle GR.

Statistical analysis

Comparison of enzyme kinetics, relative protein phosphorylation and protein stability was performed using a Student's *t*-test, two-tailed, assuming unequal variances. A probability of $P<0.05$ was considered significant.

RESULTS

Purification of GR from the muscle of control and frozen frogs

The purification scheme used for wood frog muscle GR is shown in Table 1. The procedure used ion exchange chromatography on a Bio-Gel® HTP Gel hydroxyapatite column (Fig. 2A), and Cibacron Blue chromatography (Fig. 2B). GR eluted from the Cibacron Blue column at approximately 1 mol l^{-1} KCl. Frog muscle GR was purified 134.9-fold with an overall yield of activity of 34.2% (Table 1). The final specific activity of GR was 124.73 mU mg^{-1} of protein (Table 1). The success of the purification process was assessed using SDS-PAGE with Coomassie Blue staining of the gel (Fig. 3). This showed that GR was purified to near homogeneity as there was one band corresponding to the correct molecular mass of ~50 kDa for GR (Fig. 3).

Table 1. Typical purification and yield of *Rana sylvatica* muscle glutathione reductase (GR)

Purification step	Total protein (mg)	Total activity (mU)	Specific activity (mU mg^{-1})	Fold purification	Yield (%)
Crude extract	73.6	69.3	0.94	–	100
Sephadex G-50	63.6	63.0	0.99	1.1	91.0
Hydroxyapatite	0.55	25.8	46.91	49.9	37.2
Cibacron Blue	0.19	23.7	124.73	134.9	34.2

Kinetic characterization of GR

Kinetic parameters of purified muscle GR were assessed to search for differences between control and frozen animals. The K_m for GSSG and the V_{max} of GR from *R. sylvatica* muscle did not change significantly between control and frozen animals ($P>0.05$; Table 2). However, when assayed in the presence of different additives, the K_m value for GSSG did change. In the presence of 75 mmol l^{-1} urea, the K_m for GSSG increased significantly (1.57-fold, $P<0.05$) in comparison to the K_m of GSSG in untreated samples (Table 2). In contrast, in the presence of 300 mmol l^{-1} glucose, the K_m for GSSG decreased significantly to 50% of the measured K_m of GSSG in untreated samples. In the presence of both 75 mmol l^{-1} urea and 300 mmol l^{-1} glucose, the K_m for GSSG was significantly different from the K_m of GSSG in both urea-treated and -untreated samples but was not different from the K_m in the presence of glucose.

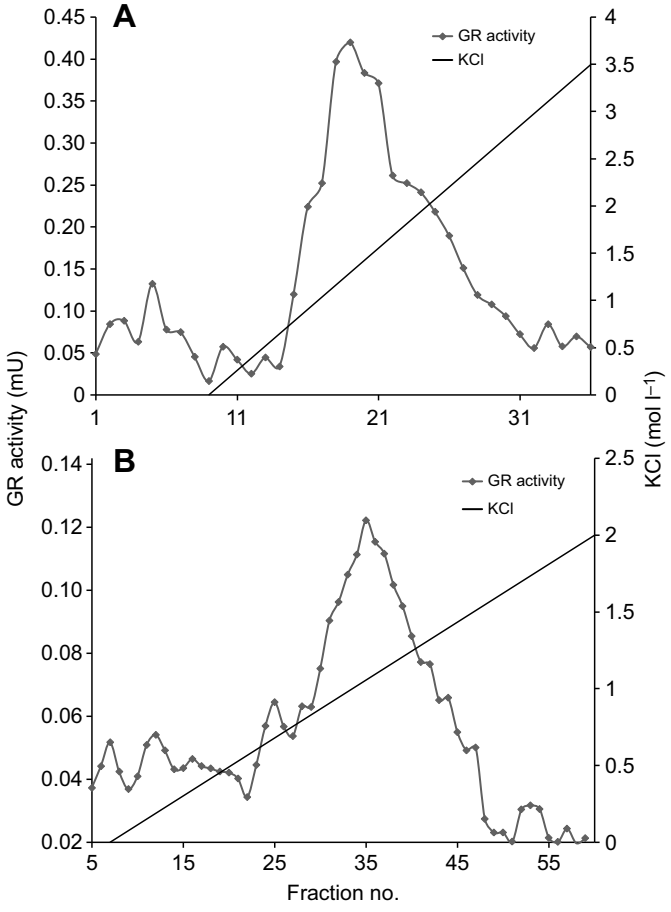

Fig. 2. Purification of GR from *R. sylvatica* muscle. (A) Typical elution profile for glutathione reductase (GR) on a hydroxyapatite column. (B) Typical elution profile for GR on a Cibacron Blue column.

Journal of Experimental Biology (2017) 220, 3162-3171 doi:10.1242/jeb.159475

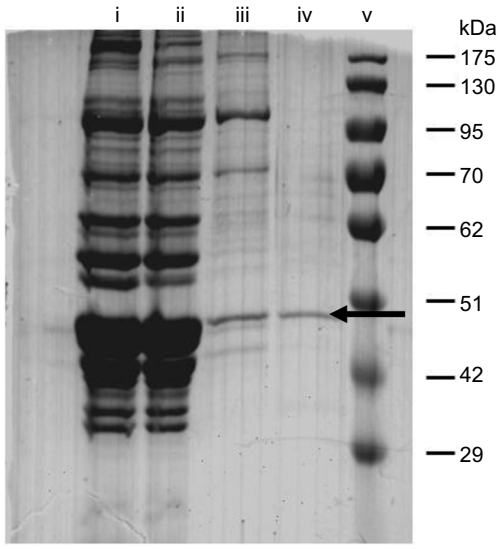

Fig. 3. Assessment of GR purification from *R. sylvatica* muscle. (i) Crude muscle homogenate. (ii) GR-containing eluant after Sephadex G-50 chromatography. (iii) GR-containing eluant after hydroxyapetite chromatography. (iv) purified GR from Cibacron Blue chromatography. (v) Molecular mass standards. GR protein is the prominent band at ~50 kDa indicated by the arrow.

GR purified from control muscle was activated when assayed in the presence of ATP (1.42-fold), ADP (1.37-fold) and AMP (1.35-fold; Table 2). K_a values for ATP and ADP were similar at 0.076 and 0.071 mmol l^{-1}, respectively. AMP had a K_a (0.16 mmol l^{-1}) more than 2-fold greater that of either ATP or ADP (Table 2).

Mn^{2+} inhibited GR activity, showing an I_{50} value (inhibitor concentration that reduced activity by 50%) of 4.44 mmol l^{-1} (Table 2). Ca^{2+} inhibited GR activity, with an I_{50} of 5.12 mmol l^{-1} (Table 2). Mg^{2+} and K^+ did not inhibit GR activity up to 10 mmol l^{-1}.

Table 2. Kinetic parameters of GR purified from muscle of control and frozen *R. sylvatica*

Enzyme parameters	Control	24 h frozen
K_m GSSG (mmol l^{-1})	0.054±0.006	0.048±0.003
V_{max} (mU g^{-1} wet mass)	125±6.1	121±5.3
T_m	63.8±0.4	64.7±0.4
K_m GSSG+urea (mmol l^{-1})	0.085±0.009*	
K_m GSSG+glucose (mmol l^{-1})	0.027±0.002*	
K_m GSSG+glucose+urea (mmol l^{-1})	0.031±0.002*	
K_a ATP (mmol l^{-1})	0.076±0.02	
Fold activation ATP	1.42	
K_a ADP (mmol l^{-1})	0.071±0.01	
Fold activation ADP	1.37	
K_a AMP (mmol l^{-1})	0.16±0.03	
Fold activation AMP	1.35	
I_{50} Mn^{2+} (mmol l^{-1})	4.44±0.33	
I_{50} Mg^{2+} (mmol l^{-1})	No inhibition ≤10 mmol l^{-1}	
I_{50} K^+ (mmol l^{-1})	No inhibition ≤10 mmol l^{-1}	
I_{50} Ca^{2+} (mmol l^{-1})	5.12±0.99	
E_a (kJ mol^{-1})	40.7±0.9	

To test the effects of additives on K_m, assays were run with the addition of 75 mmol l^{-1} urea or 300 mmol l^{-1} glucose. K_a and I_{50} values were determined at K_m values for GSSG. Values are means±s.e.m. (n=8).
*Significantly different from the corresponding K_m value for GSSG in the absence of glucose or urea (Student's t-test; P<0.05).

Post-translational modification of GR

To test whether GR was susceptible to reversible phosphorylation, the purified GR from muscle of both control and frozen frogs was run on an SDS-PAGE gel and stained with Pro-Q Diamond phosphoprotein stain. GR did not react with the Pro-Q Diamond phosphoprotein stain, resulting in no apparent banding (Fig. 4A).

Crude extracts of skeletal muscle from control and frozen frogs were incubated to stimulate the activity of endogenously present kinases and GR was then purified. The enzyme showed a clear band at ~50 kDa when stained for total phosphorylation (Fig. 4B). However, there was no significant difference in band intensity between GR purified from control and frozen samples.

Immunoblotting was used to assess residue-specific phosphorylation of muscle GR. Purified GR reacted with antibodies testing for phosphorylation on serine residues, threonine residues and tyrosine residues (Fig. 5). However, relative phosphorylation levels of serine, threonine and tyrosine residues did not change between control and frozen states (P>0.05).

Scansite prediction of phosphosites

The Scansite application from the Massachusetts Institute of Technology (http://scansite.mit.edu/) was used to analyze GR sequences from two other frogs, *X. laevis* and *X. tropicalis*, to search the proteins for putative phosphorylation sites (Fig. 6). GR protein sequences showed 94.75% identity between *X. tropicalis* and *X. laevis*. Multiple putative phosphorylation sites were predicted to occur on GR based on the presence of consensus sequence motifs for different protein kinases. Only those kinases predicted to phosphorylate GR from both *X. laevis* and *X. tropicalis* are reported. Putative consensus sequences for phosphorylation sites of Akt kinase (protein kinase B; threonine), AMPK (serine, threonine), CaMKII (serine, threonine), casein kinase 1 (CK1; serine, threonine), casein kinase 2 (CK2; serine, threonine), epidermal growth factor receptor kinase (EGFR; tyrosine), Fgr kinase (tyrosine), insulin receptor kinase (tyrosine), PKA (serine,

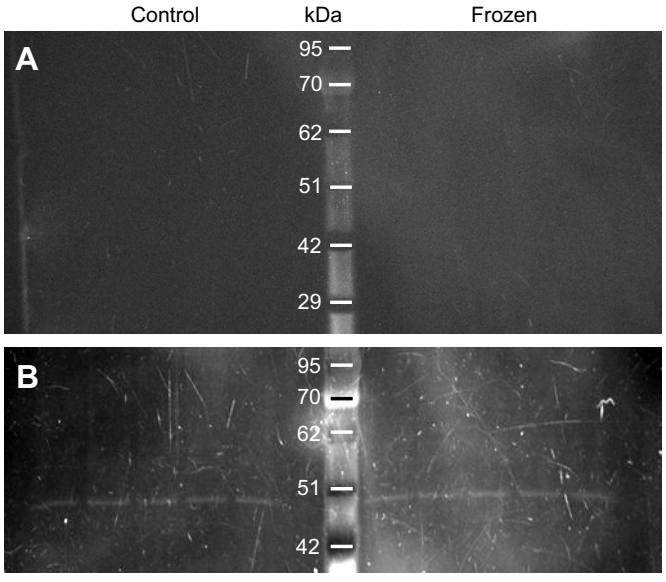

Fig. 4. Phosphorylation of GR in control and frozen muscle. (A) The absence of bands indicates no apparent phosphorylation of muscle GR from either control or 24 h frozen frogs as assessed by Pro-Q diamond phosphoprotein staining. (B) Relative phosphorylation levels of GR from control and 24 h frozen frog muscle after total kinase incubations as assessed by Pro-Q diamond phosphoprotein staining.

Journal of Experimental Biology

Journal of Experimental Biology (2017) 220, 3162-3171 doi:10.1242/jeb.159475

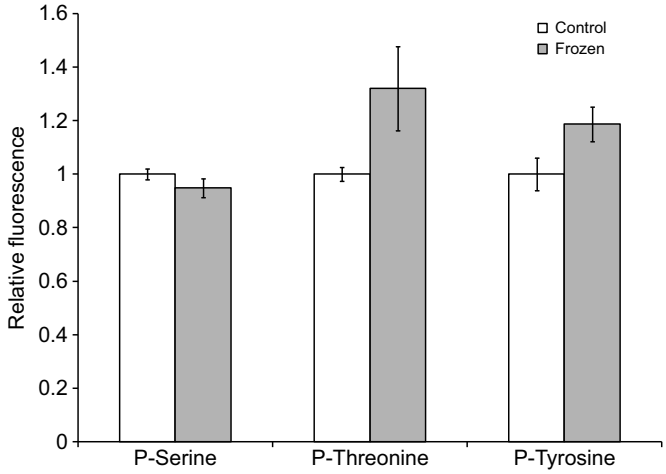

Fig. 5. Relative phosphorylation levels of frog muscle GR after incubation to stimulate total kinases. Residue-specific phosphorylation of GR from control and frozen muscle was compared using western blot analysis. There were no significant differences between control and frozen values (Student's *t*-test; $P<0.05$). Values are means±s.e.m. ($n=8$).

threonine), PKCα (serine, threonine), PKCβ (serine, threonine), PKCδ (serine), PKCε (serine), PKCγ (serine, threonine) and PKCμ (serine) were predicted for GR (Fig. 6B).

Human GR shows 81.75% identity to *X. laevis* and *X. tropicalis* GR. Human GR was analyzed for comparison using Scansite, resulting in the following putative consensus sequences for phosphorylation sites: Akt kinase (serine, threonine), AMPK (serine, threonine), CaMKII (serine), CK1 (threonine), CK2 (threonine), EGFR kinase (tyrosine), extracellular signal-regulated kinase 1 (Erk1; serine, threonine), Fgr kinase (tyrosine), glycogen synthase kinase 3 (GSK3; serine, threonine), insulin receptor kinase (tyrosine), PKA (threonine), PKCα (serine, threonine), PKCβ (serine, threonine), PKCδ (serine, threonine), PKCε (threonine), PKCγ (serine, threonine), PKCμ (serine, threonine) and PKCζ (serine) were predicted for GR.

Arrhenius plots

Maximum GR activity was measured at 5°C increments starting from 5°C and ending at 45°C using purified GR from the leg muscle of *R. sylvatica*. Purified GR demonstrated a positive correlation between temperature and activity (Fig. 7). Arrhenius plots were created by plotting $\ln(V_{max})$ versus 1/temperature (in K). The E_a was then calculated as 40.7±0.9 kJ mol^{-1} (Table 2, Fig. 7).

Stability of GR

The structural stability of GR was evaluated by testing enzyme sensitivity to thermal denaturation using differential scanning fluorimetry. There was no significant difference in the pattern of thermal denaturation of purified GR between control and frozen frogs (Fig. 8). GR purified from the muscle of *R. sylvatica* showed a peak at 68°C for both control and frozen frogs. The calculated T_m value (the temperature that results in a 50% loss of folded enzyme) was 64.7°C for GR from control frog muscle extracts, which was not significantly different from the value of 63.8°C for GR from frozen muscle extracts (Table 2, Fig. 8).

DISCUSSION

Abnormalities in GR activity have been linked to disease states including Parkinson's disease and Alzheimer's disease, in which an increase in GSSG concentration was linked with greater apoptotic cell death (Merad-Boudia et al., 1998; Aksenov and Markesbery, 2001; Diaz-Hernandez et al., 2005). An increase in the activity of GR has been observed in rheumatoid arthritis (Mulherin et al., 1996), and changes in the expression level and activity of GR have also been found in cancer (Mullineaux and Creissen, 1997). Although the exact role of GR in disease is still being explored, knockout and knockdown experiments with GR have proved to be lethal (Pretsch, 1999; Rogers et al., 2004, 2006). Specifically, elevated levels of GSSG due to oxidative stress have been directly linked to apoptotic signaling events in these experiments. As the function of GR seems paramount for the continued survival and quality of life in humans, exploration of GR function in organisms than can endure long periods of time under conditions that mimic disease-like states is of great interest to understanding the role of GR in disease. A common theme observed for the diseases mentioned above is an increase in oxidative stress imposed on both the whole cell and at the mitochondrial level due to fluctuations in blood flow and oxygen deprivation. Organisms experiencing changes in GR regulation under oxygen-deprived states include: the red eared slider turtle (*Trachemys scripta elegans*), which shows fluctuations in GR activity as well as decreased GSH levels in the liver, heart and muscle during anoxia (Willmore and Storey, 1997), the leopard frog (*Rana pipiens*), which shows a reduction in GR activity in muscle tissue during severe dehydration (Hermes-Lima and Storey, 1998), the common carp (*Cyprinus carpio*), which shows increases in GR activity in the brain during hypoxia (Lushchak et al., 2005), the spadefoot toad (*Scaphiopus couchii*), where GR activity in the liver, heart and kidney was significantly lower during estivation (Grundy and Storey, 1998), and the marine periwinkle (*Littorina littorea*), where GR activity decreased in the hepatopancreas during anoxia as well as foot muscle upon exit from anoxia (Pannunzio and Storey, 1998).

In line with the animals discussed above, the freeze-tolerant frog also experiences low oxygen, specifically in the form of ischemia, which has been repeatedly demonstrated to include oxidative stress and a burst production of ROS in the reperfusion recovery episode (Ferrari et al., 1991; Simpson and Lucchesi, 1987; Zweier and Talukder, 2006). In contrast to the other animals, the freeze-tolerant frog controls freezing and limits dehydration and cellular damage through the accumulation of cryoprotectants, primarily glucose and urea (Storey and Storey, 1984; Costanzo et al., 1993; Costanzo and Lee, 1993; Muir et al., 2008; Schiller et al., 2008). This provides the frog with a unique advantage in that glucose is widely thought of as a protein stabilizer which may aid protein function during the frozen state (Imamura et al., 2003; Biggar et al., 2012; Childers et al., 2016); however, elevated levels of glucose are linked to increased oxidative stress, while urea is a commonly used as a protein denaturant (Bonnefont-Rousselot, 2002; Biggar et al., 2012; Childers et al., 2016; Dawson et al., 2015). Additionally, previous specializations in the antioxidant defense system have been reported in *R. sylvatica*, involving improved function of MnSOD and catalase during the frozen state (Dawson et al., 2015, Dawson and Storey, 2016); however, little is known about the effects of freezing on glutathione reductase. Studies involving the overexpression or increased activity of GR in the mitochondria have shown increased resistance to oxidative stress (Foyer et al., 1995; Mockett et al., 1999). Therefore, through exploration of the role of GR in maintaining GSH pools during freezing in *R. sylvatica*, with particular emphasis on the effects of cryoprotectants on GR function, the regulation of GR in the frozen frog can provide important information for both the survival of the animal upon exit

Journal of Experimental Biology (2017) 220, 3162-3171 doi:10.1242/jeb.159475

A

X tropicalis	MHKPASDSPS GNGHLPRYYD **Y**LVVGGGSGG LASARRAAEL GARTAVVE**S**S KLGGTCVNVG	60
X laevis	MHKPVPDSHS SDGHLPRYFD **Y**LVVGGGSGG LASARRAAEL GARTAVVE**S**S KLGGTCVNVG	60
X tropicalis	CVPKKIMWNA AMHSEYIHDH ADYGFEIPDV KFTWKVIKEK RDAYVSRLND IYQNNLQKAQ	120
X laevis	CVPKKIMWNA AIHSEYIHDH EDYGFETSAI KFTWKVIKEK RDAYVSRLND IYQNNLQKAQ	120
X tropicalis	IEIIRGNANF TSDPEPTVEV NGQKYSAPHI LIATGGKPSM PSDAELPGAS LGITSDGFFE	180
X laevis	IEIIRGQANF TSDSEPTVEV NGQKYIAPHI LIATGGKPSM PSDAEVPGAS LGITSDGFFQ	180
X tropicalis	LTDLPRR**S**IV VGAGYIAVEI AGILSALGSK A**S**LLIRQDKV LRTFDSIISS NC**T**EELENAG	240
X laevis	LTDLPRR**S**VV VGAGYIAIEI AGILSALGSK A**S**LLIRQDKV LRTFDSMISS NC**T**EELENAG	240
X tropicalis	VEVWKYAQVK **S**VKKST**T**GLE INVQCSMPGR KP**T**VRTIQDV DCLLWAIGRD PNTEYLGLEN	300
X laevis	VEVWKYAQVK **S**VKKSA**T**GLE INVQCSMPGR KP**T**VRTIQDV DCLLWAIGRD PNTEDLGLEN	300
X tropicalis	LGLELDEKGH IVVDEFQNTS RKGVYAVGDV CGRALLTPVA IAAGRKL**S**HR LFEGQEDSKL	360
X laevis	LGLELDEKGH IVVDEFQNTS RKGVYAVGDV CGRALLTPVA IAAGRKL**S**HR LFEGQEDSKL	360
X tropicalis	DYNNIPTVVF SHPPIGTVGL **T**EEEAV**T**AKG RENVKVYTTS FSPMYHVVTR RK**T**KCVMKLV	420
X laevis	DYDNIPTVVF SHPPIGTVGL **T**EEEAV**T**AKG RENVKVYTTS FSPMYHAVTR RK**T**KCVMKLV	420
X tropicalis	CVGKEEKVVG LHMQGLGCDE MLQGFAVAIK MGATKKDFDN TVAIHPTSSE ELVTLR	476
X laevis	CVGKEEKVVG LHMQGLGCDE MLQGFSVAIK MGATKKDFDN TVAIHPTSSE ELVTLR	476

B

S49 – PKCδ
S188 – PKA
S212 – AMPK, CK1, PKCα/β/γ/μ
S251 – CK1, PKCα/β/γ/ε/δ
S348 – CaMKII, PKA

T223 – CaMKII, CK2
T257 – AMPK
T273 – Akt kinase, PKA, PKCα/β/γ
T381 – Erk1 kinase 2
T387 – PKA
T413 – PKA

Y21 – EGFR, Fgr kinase, Insulin receptor kinase

Fig. 6. Predicated phosphorylation sites on GR. (A) Comparison of the predicted serine (S), threonine (T) and tyrosine (Y) phosphorylation sites on GR that are shared between *Xenopus tropicalis* and *Xenopus laevis*. Predicted phosphorylation sites are shown in bold and underlined. (B) Specific kinases predicted to phosphorylate the highlighted phosphorylation sites. PKC, protein kinase C; PKA, protein kinase A; AMPK, AMP-activated protein kinase; Akt, protein kinase B; Erk, extracellular signal-regulated kinase; EGFR, epidermal growth factor receptor.

from the frozen state and insight into disease states that could possibly benefit from a similar regulation of GR to stave off apoptosis upon reoxygenation following ischemia.

Kinetic changes of GR in the face of increasing glucose

The kinetic properties of wood frog skeletal muscle GR were not significantly different for GR purified from control and frozen animals (Table 2). As GR is an abundant enzyme in muscle cells, and is found in several subcellular locations, it may be less energetically costly to modify the entire GR pool in order to deal with the stress imposed by freezing. However, covalent modification of proteins is only one of many methods to change enzyme activity or function. *Rana sylvatica* increases the levels of select osmolytes to extreme values during freezing (e.g.

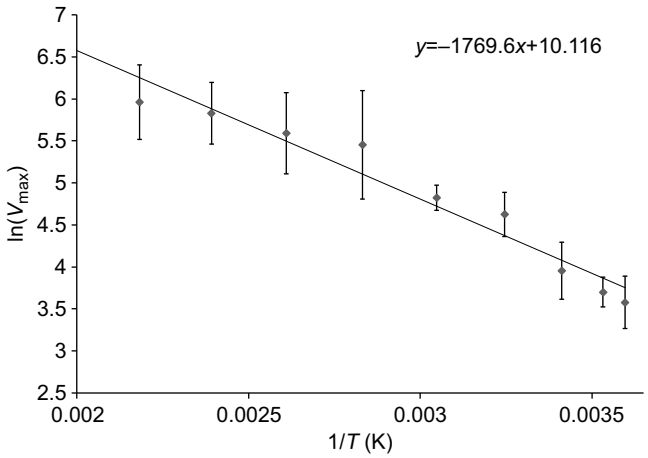

Fig. 7. Arrhenius plot for purified GR from the muscle of control *R. sylvatica*. Activity [ln(V_{max})] is plotted against the inverse of temperature (T). Values are means±s.e.m. (n=8).

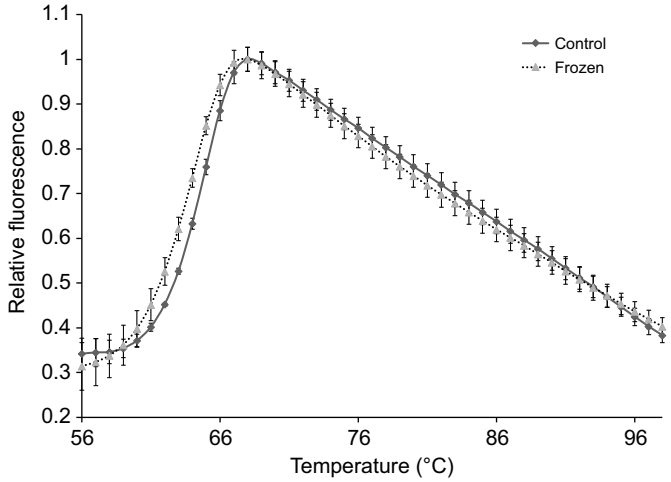

Fig. 8. Thermal stability of GR from control and frozen muscle. Stability was assessed by differential scanning fluorimetry analysis. The stability of GR from frozen frogs showed no significant difference from that of GR from control frogs (Student's t-test; P<0.05). Values are means±s.e.m. (n=8).

Journal of Experimental Biology (2017) 220, 3162-3171 doi:10.1242/jeb.159475

>200 mmol l^{-1} glucose), which seems to affect the enzymatic function of GR (Storey and Storey, 2004).

GR purified from the muscle of *R. sylvatica* demonstrated significant changes in affinity for GSSG when tested in the presence of the physiological concentrations of glucose or urea that are encountered during freezing (Table 2). GR showed a significant decrease in affinity for GSSG when subjected to physiological levels of urea (75 mmol l^{-1}) that can be present during freezing (Table 2). This phenomenon was overwhelmed by the effects of high glucose, as purified GR showed a significant increase in affinity for GSSG when subjected to physiological levels of glucose alone or glucose+urea (Table 2). As previously mentioned, *R. sylvatica* elevates glucose levels in order to prevent the osmotic loss of water from cells due to freezing of extracellular water. The frog may be benefitting from a pre-existing hyperglycemic response to augment the function of GR.

Ischemia stress must be removed in order to return glucose levels to normal; therefore, the positive effects of glucose on GR activity would likely remain throughout the burst production of ROS during reperfusion. Once the initial oxidative stress imposed on the cells as a result of prolonged ischemia has been surmounted, glucose levels will gradually return to normal levels, and the glucose-induced increase in GR affinity for GSSG will also return to normal. This is of note, as the GSSG/GSH ratio is involved in many signaling pathways, and could be disrupted by maintaining elevated GR affinity beyond the necessary time to overcome reperfusion-induced ROS production.

In humans, high glucose has been suggested to increase the production of free radicals, and ultimately cell death and reduced proliferation, in diabetic and glucose-treated human cell lines (Durante et al., 1988; Curcio and Ceriello, 1992; Tesfamariam and Cohen, 1992; Ceriello et al., 1996). However, elevated or added GSH has demonstrated protective effects on glucose-treated human cell lines (Marfella et al., 1995). Previous studies on the effects of elevated glucose levels on antioxidant enzymes have demonstrated up-regulation in the presence of high glucose, suggesting that glucose can stimulate the activity of antioxidant enzymes (Ceriello et al., 1996). It is clear from these studies, as well as the evidence of glucose-activated GR found here, that glucose levels, free radicals and antioxidant enzyme activity are linked.

Kinetic changes of GR due to common metabolites

The effect of Ca^{2+} on GR is likely linked to damage of the mitochondrial membrane, which would lead to an increase in the cytoplasmic Ca^{2+} concentration (Halliwell, 1992). Leakage of Ca^{2+} has been widely characterized in the mitochondrial signaling of apoptosis (Pinton et al., 2008). It has also been suggested that freeze–thaw cycles can disrupt Ca^{2+} transport in muscle, suggesting that as Ca^{2+} levels return to normal, GR activity could be influenced by the change in Ca^{2+} levels (Halliwell, 1992; Storey and Storey, 2004).

Cellular Mn^{2+} exists mainly in complexes with proteins, and a rise in free metals is usually the result of damage to proteins and the subsequent release of the bound metals from the protein structure (Valko et al., 2005). It would appear that the inhibition of GR is linked to cellular damage and subsequent release of Mn^{2+} when proteins are damaged; however, it is unclear at this time what the role of Mn^{2+} is in inhibiting GR activity in *R. sylvatica*.

Rana sylvatica ATP levels have been shown to drop in some tissues during freezing (Storey and Storey, 1984). However, ATP, ADP and AMP were observed to activate GR similarly (Table 2), suggesting that any activation of GR by changes in adenylate ratios during freezing is unlikely.

Phosphorylation of GR during freezing and induced phosphorylation of GR by endogenous kinases

Reversible protein phosphorylation has been demonstrated as an important method of modifying key enzymes involved in the success of *R. sylvatica* during freezing (Dieni and Storey, 2008, 2009, 2010, 2011; Abboud and Storey, 2013; Dawson et al., 2015; Dawson and Storey, 2016). The potential phosphorylation of GR during freezing was therefore explored in order to determine whether this same method of regulation is used to aid GSSG/GSH homeostasis during freezing. However, there was no evidence of changes in the phosphorylation state of GR between control or frozen states as assessed by Pro-Q Diamond staining (Fig. 4). This lack of phosphorylation suggested that any differences in GR activity are not due to a freeze-induced phosphorylation event.

The phosphorylation state of GR was nonetheless explored as a potential method of further regulating the protein and to discover whether different phosphorylation profiles are possible between the control and frozen states. The activities of endogenous kinases were stimulated in frog muscle homogenates, resulting in the phosphorylation of frog muscle GR (Fig. 4B). Fig. 1 shows the elution profile for control and frozen preparations from a $DEAE^{+}$ column. There was no significant difference in the elution profiles, suggesting that no frozen state-specific phosphorylation event occurred. Further analysis of the induced phosphorylation of GR suggested that phosphorylation was achieved on serine, threonine and tyrosine residues (Fig. 5). This is the first study to show phosphorylation of GR *in vitro*.

However, phosphorylation of GR does not seem to play a role in freeze tolerance of *R. sylvatica*, although it highlights the propensity of GR for phosphorylation, which may play other roles in the regulation of GR in the frog. Investigation based on GR sequences from *X. laevis* and *X. tropicalis* showed the presence of putative sites for serine, threonine and tyrosine kinases, supporting the notion that endogenous kinases in *R. sylvatica* muscle can phosphorylate GR (Fig. 6). Several of the kinases stimulated in the endogenous incubation study were among those predicted to phosphorylate GR, including AMPK, CaMK, PKA and PKC. This suggests that although altered phosphorylation of GR is not a factor in the freeze tolerance of *R. sylvatica*, it could play a role in other cellular functions. Interestingly, human GR also shows potential serine, threonine and tyrosine phosphorylation sites, suggesting the possibility for GR phosphorylation in humans. Although GR shows a propensity for phosphorylation, more work must be conducted to elucidate the physiological role of phosphorylation of this enzyme. It is clear, however, that the phosphorylation of GR during freezing in *R. sylvatica* is unlikely to have a role in the maintenance of the GSH/GSSG levels.

Thermal stability and temperature-dependent activity of GR

GR purified from both control and frozen frogs was explored via differential scanning fluorimetry, and showed no significant differences in enzyme structural stability between states (Fig. 8). This provides further proof that GR from control and frozen animals is not functionally different. Past studies of GR have demonstrated the thermodynamic stability of GR activity, and have similarly shown that GR remains active across a broad range of temperatures (Lopez-Barea and Chi-Yu, 1979; Ohtsuka et al., 1994; Rescigno and Perham, 1994). The T_m determined for frog GR shows that denaturation takes place at a relatively high temperature of

approximately 64°C, suggesting the GR is a very stable enzyme (Table 2, Fig. 8). The calculated E_a was 40.7 kJ mol^{-1}, which suggests that the reaction catalyzed by GR is endothermic in nature, and that the reaction may be hindered at low temperatures.

Conclusions

This study of the regulation of GR in the freeze-tolerant frog *R. sylvatica* provides useful insights into the maintenance of the cellular redox states as well as the GSSG/GSH ratios involved in apoptotic cell signaling. The regulation of GR activity during freezing seems to be related to the changing cellular environment, specifically increases in glucose concentrations. GR from *R. sylvatica* seems to have coupled an increase in the affinity for GSSG with a natural increase in the concentration of glucose during freezing. Although cytosolic concentrations of GSH are significantly higher in *R. sylvatica* than in other closely related frog species, an increase in GR activity may be vital to maintaining GSH/GSSG levels, specifically in the mitochondria. The mitochondrial production of ROS has been linked to apoptotic signaling, and GR activity may be augmented in order to combat the mitochondrial production of ROS during thaw-induced reperfusion. GR, along with many antioxidant-related proteins, has a high degree of similarity across species. The similarity observed in mitochondrial proteins could allow for researchers to explore possible roles for GR in a controlled ischemic state, such as freezing in *R. sylvatica*. It is clear from this study and others that the role of GSH and GR maintenance of the mitochondrial redox environment during freezing in *R. sylvatica* should be explored in greater detail, as it could provide valuable insight into disease pathology by offering an alternative perspective on the role of GR during ischemia.

Acknowledgements

The authors thank J. M. Storey for assistance in editing the manuscript.

Competing interests

The authors declare no competing or financial interests.

Author contributions

Conceptualization: N.J.D., K.B.S.; Methodology: N.J.D.; Validation: N.J.D., K.B.S.; Formal analysis: N.J.D.; Investigation: N.J.D.; Resources: K.B.S.; Data curation: N.J.D.; Writing - original draft: N.J.D.; Writing - review & editing: N.J.D., K.B.S.; Visualization: N.J.D.; Supervision: K.B.S.; Project administration: N.J.D.; Funding acquisition: K.B.S.

Funding

This research was supported by a discovery grant from the Natural Sciences and Engineering Research Council of Canada (no. 6793) to K.B.S. N.J.D. was supported by an Ontario Graduate Scholarship.

References

Abboud, J. and Storey, K. B. (2013). Novel control of lactate dehydrogenase from the freeze tolerant wood frog: role of posttranslational modifications. *Peer J.* **1**, e12.

Aksenov, M. Y. and Markesbery, W. R. (2001). Changes in thiol content and expression of glutathione redox system genes in the hippocampus and cerebellum in Alzheimer's disease. *Neurosci. Lett.* **302**, 141-145.

Armstrong, J. S. Steinauer, K. K., Hornung, B., Irish, J. M., Lecane, P., Birrell, G. W., Peehl, D. M. and Knox, S. J. (2002). Role of glutathione depletion and reactive oxygen species generation in apoptotic signaling in a human B lymphoma cell line. *Cell Death Differ.* **9**, 252-263.

Biggar, K. K., Dawson, N. J. and Storey, K. B. (2012). Real-time protein unfolding: a method for determining the kinetics of native protein denaturation using a quantitative real-time thermocycler. *BioTechniques* **53**, 231-238.

Bonnefont-Rousselot, D. (2002). Glucose and reactive oxygen species. *Curr. Opin. Clin. Nutr. Metab. Care.* **5**, 561-568.

Brooks, S. P. (1992). A simple computer program with statistical tests for the analysis of enzyme kinetics. *BioTechniques* **13**, 906-911.

Ceriello, A., dello Russo, P., Amstad, P. and Cerutti, P. (1996). High glucose induces antioxidant enzymes in human endothelial cells in culture: evidence linking hyperglycemia and oxidative stress. *Diabetes* **45**, 471-477.

Childers, C. L., Green, S. R., Dawson, N. J. and Storey, K. B. (2016). Native denaturation differential scanning fluorimetry: determining the effect of urea using a quantitative real-time thermocycler. *Anal. Biochem.* **508**, 114-117.

Circu, M. L. and Aw, T. Y. (2008). Glutathione and apoptosis. *Free Radic. Res.* **42**, 689-706.

Costanzo, J. P. and Lee, E. E.Jr. (1993). Cryoprotectant production capacity of the freeze-tolerant wood frog, *Rana sylvatica*. *Can. J. Zool.* **71**, 71-75.

Costanzo, J. P., Lee, E. E. and Lortz, P. H. (1993). Glucose concentration regulates freeze tolerance in the wood frog *Rana sylvatica*. *J. Exp. Biol.* **181**, 245-255.

Cowan, K. J. and Storey, K. B. (2001). Freeze-thaw effects on metabolic enzymes in wood frog organs. *Cryobiology* **43**, 32-45.

Curcio, F. and Ceriello, A. (1992). Decreased cultured endothelial cell proliferation in high glucose medium is reversed by antioxidants: new insights on the pathophysiological mechanism of diabetic vascular complications. *In Vitro Cell. Dev. Biol.* **28**, 787-790.

Dawson, N. J. and Storey, K. B. (2016). A hydrogen peroxide safety valve: the reversible phosphorylation of catalase from the freeze-tolerant North American wood frog, *Rana sylvatica*. *Biochim. Biophys. Acta.* **1860**, 476-485.

Dawson, N. J., Katzenback, B. A. and Storey, K. B. (2015). Free-radical first responders: the characterization of CuZnSOD and MnSOD regulation during freezing of the freeze-tolerant North American wood frog, *Rana sylvatica*. *Biochim. Biophys. Acta.* **1850**, 97-106.

Di Ilio, C., Polidoro, G., Arduini, A., Muccini, A. and Federici, G. (1983). Glutathione peroxidase, glutathione reductase, glutathione S-transferase, and γ-glutamyltranspeptidase activities in the human early pregnancy placenta. *Biochem. Med.* **29**, 143-148.

Diaz-Hernandez, J. I., Almeida, A., Delgado-Esteban, M., Fernandez, E. and Bolaños, J. P. (2005). Knockdown of glutamate-cysteine ligase by small hairpin RNA reveals that both catalytic and modulatory subunits are essential for the survival of primary neurons. *J. Biol. Chem.* **280**, 38992-39001.

Dieni, C. A. and Storey, K. B. (2008). Regulation of 5'-adenosine monophosphate deaminase in the freeze tolerant wood frog, *Rana sylvatica*. *BMC Biochem.* **9**, 12.

Dieni, C. A. and Storey, K. B. (2009). Creatine kinase regulation by reversible phosphorylation in frog muscle. *J. Comp. Biochem. Physiol. B.* **152**, 405-412.

Dieni, C. A. and Storey, K. B. (2010). Regulation of glucose-6-phosphate dehydrogenase by reversible phosphorylation in liver of a freeze tolerant frog. *J. Comp. Physiol. B.* **180**, 1133-1142.

Dieni, C. A. and Storey, K. B. (2011). Regulation of hexokinase by reversible phosphorylation in skeletal muscle of a freeze tolerant frog. *Comp. Biochem. Physiol. B.* **159**, 236-243.

Durante, W., Sen, A. K. and Sunahara, F. A. (1988). Impairment of endothelium-dependent relaxation in aortae from spontaneously diabetic rats. *Br. J. Pharmacol.* **94**, 463-468.

Ferrari, R., Ceconi, C., Curello, S., Cargnoni, A., Pasini, E., De Giuli, F. and Albertini, A. (1991). Role of oxygen free radicals in ischemic and reperfused myocardium. *Am. J. Clin. Nutrit.* **53**, 215S-222S.

Forman, H. J., Zhang, H. and Rinna, A. (2009). Glutathione: overview of its protective roles, measurement, and biosynthesis. *Mol. Aspects Med.* **30**, 1-12.

Foyer, C. H., Souriau, N., Perret, S., Lelandais, M., Kunert, K. J., Pruvost, C. and Jouanin, L. (1995). Overexpression of glutathione reductase but not glutathione synthetase leads to increases in antioxidant capacity and resistance to photoinhibition in poplar trees. *Plant Phys.* **109**, 1047-1057.

Franco, R. and Cidlowski, J. A. (2009). Apoptosis and glutathione: beyond an antioxidant. *Cell Death Differ.* **16**, 1303-1314.

Friesen, C., Kiess, Y. and Debatin, K.-M. (2004). A critical role of glutathione in determining apoptosis sensitivity and resistance in leukemia cells. *Cell Death Differ.* **11**, S73-S85.

Galluzzi, L., Maiuri, M. C., Vitale, I., Zischka, H., Castedo, M., Zitvogel, L. and Kroemer, G. (2007). Cell death modalities: classification and pathophysiological implications. *Cell Death Differ.* **14**, 1237-1243.

Garcia-Ruiz, C. and Fernandez-Checa, J. C. (2006). Mitochondrial glutathione: hepatocellular survival death switch. *J. Gastroenterol. Hepatol.* **21**, S3-S6.

Grundy, J. E. and Storey, K. B. (1998). Antioxidant defenses and lipid peroxidation damage in estivating toads, *Scaphiopus couchii*. *J. Comp. Physiol. B.* **168**, 132-142.

Halliwell, B. (1992). Reactive oxygen species and the central nervous system. *J. Neurochem.* **59**, 1609-1623.

Hermes-Lima, M. and Storey, K. B. (1998). Role of antioxidant defenses in the tolerance of severe dehydration in anurans. The case of the leopard frog Rana pipiens. *Mol. Cell. Biochem.* **189**, 79-89.

Imamura, K., Ogawa, T., Sakiyama, T. and Nakanishi, K. (2003). Effects of types of sugar on the stabilization of protein in the dried state. *J. Pharm. Sci.* **92**, 266-274.

Joanisse, D. R. and Storey, K. B. (1996). Oxidative damage and antioxidants in *Rana sylvatica*, the freeze-tolerant wood frog. *Am. J. Physiol.* **271**, R545-R553.

Klein, S. L., Strausberg, R. L., Wagner, L., Pontius, J., Clifton, S. W. and Richardson, P. (2002). Genetic and genomic tools for *Xenopus* research: the NIH Xenopus initiative. *Dev. Dyn.* **225**, 384-391.

Krauth-Siegel, R. L., Arscott, L. D., Schönleben-Janas, A., Schirmer, R. H. and Williams, C. H. (1998). Role of active site tyrosine residues in catalysis by human glutathione reductase. *Biochemistry* **37**, 13968-13977.
Lash, L. H. (2006). Mitochondrial glutathione transport: physiological, pathological and toxicological implications. *Chem. Biol. Interact.* **163**, 54-67.
Lopez-Barea, J. and Lee, C.-Y. (1979). Mouse-liver glutathione reductase. *Eur. J. Biochem.* **98**, 487-499.
Lushchak, V. I., Bagnyukova, T. V., Lushchak, O. V., Storey, J. M. and Storey, K. B. (2005). Hypoxia and recovery perturb free radical processes and antioxidant potential in common carp (*Cyprinus carpio*) tissues. *Int. J. Biochem. Cell. Biol.* **37**, 1319-1330.
MacDonald, J. A. and Storey, K. B. (1999). Regulation of ground squirrel Na+ K+-ATPase activity by reversible phosphorylation during hibernation. *Biochem. Biophys. Res. Comm.* **254**, 424-429.
Marchetti, P., Decaudin, D., Macho, A., Zamzami, N., Hirsch, T., Susin, S. A. and Kroemer, G. (1997). Redox regulation of apoptosis: impact of thiol oxidation status on mitochondrial function. *Eur. J. Immunol.* **27**, 289-296.
Marfella, R., Verrazo, G., Acampora, R., La Marca, C., Giunta, R., Lucarelli, C., Paolisso, G., Ceriello, A. and Giugliano, D. (1995). Glutathione reverses systemic hemodynamic changes induced by acute hyperglycemia in healthy subjects. *Am. J. Physiol.* **268**, E1167-E1173.
Meister, A. (1995). Glutathione biosynthesis and its inhibition. *Methods Enzymol.* **252**, 26-30.
Merad-Boudia, M., Nicole, A., Santiard-Baron, D., Saille, C. and Ceballos-Picot, I. (1998). Mitochondrial impairment as an early event in the process of apoptosis induced by glutathione depletion in neuronal cells: relevance to Parkinson's disease. *Biochem. Pharmacol.* **56**, 645-655.
Meyer, Y., Buchanan, B. B., Vignols, F. and Reichheld, J.-P. (2009). Thioredoxins and glutaredoxins: unifying elements in redox biology. *Annu. Rev. Genet.* **43**, 335-367.
Mockett, R. J., Sohal, R. S. and Orr, W. C. (1999). Overexpression of glutathione reductase extends survival in transgenic *Drosophila melanogaster* under hyperoxia but not normoxia. *FASEB J.* **13**, 1733-1742.
Muir, T. J., Costanzo, J. P. and Lee, R. E., Jr. (2008). Metabolic depression induced by urea in organs of the wood frog, *Rana sylvatica*: effects of season and temperature. *J. Exp. Zool.* **309**, 111-116.
Mulherin, D. M., Thurnham, D. I. and Situnayake, R. D. (1996). Glutathione reductase activity, riboflavin status, and disease activity in rheumatoid arthritis. *Ann. Rheum. Dis.* **55**, 837-914.
Mullineaux, P. and Creissen, G. P. (1997). Glutathione reductase: regulation and role in oxidative stress. In *Oxidative Stress and the Molecular Biology of Antioxidant Defences* (ed. J. G. Scandalios), pp. 667-713. Cold Spring Harbor: Monograph.
Muyderman, H., Wadey, A. L., Nilsson, M. and Sims, N. R. (2007). Mitochondrial glutathione protects against cell death induced by oxidative and nitrative stress in astrocytes. *J. Neurochem.* **102**, 1369-1382.
Niesen, F. H., Berglund, H. and Vedadi, M. (2007). The use of differential scanning fluorimetry to detect ligand interactions that promote protein stability. *Nat. Protoc.* **2**, 2212.
Ohtsuka, Y., Yabunaka, N., Fujisawa, H., Watanabe, I. and Agishi, Y. (1994). Effect of thermal stress on glutathione metabolism in human erythrocytes. *Eur. J. Appl. Physiol. Occup. Hysiol.* **68**, 87-91.
Pannunzio, T. M. and Storey, K. B. (1998). Antioxidant defenses and lipid peroxidation during anoxia stress and aerobic recovery in the marine gastropod *Littorina littorea*. *J. Exp. Mar. Biol. Ecol.* **221**, 277-292.
Pinton, P., Giorgi, C., Siviero, R., Zecchini, E. and Rizzuto, R. (2008). Calcium and apoptosis: ER-mitochondria Ca^{2+} transfer in the control of apoptosis. *Oncogene* **27**, 6407-6418.
Pretsch, W. (1999). Glutathione reductase activity deficiency in homozygous $Gr1^{a1Neu}$ mice does not cause haemolytic anaemia. *Genet. Res.* **73**, 1-5.
Rescigno, M. and Perham, R. N. (1994). Structure of the NADPH-Binding motif of glutathione reductase: efficiency determined by evolution. *Biochemistry.* **33**, 5721-5727.
Rogers, L. K., Tamura, T., Rogers, B. J., Welty, S. E., Hansen, T. N. and Smith, C. V. (2004). Analyses of glutathione reductase hypomorphic mice indicate a genetic knockout. *Toxicol. Sci.* **82**, 367-373.
Rogers, L. K., Bates, C. M., Welty, S. E. and Smith, C. V. (2006). Diquat induces renal proximal tubule injury in glutathione reductase-deficient mice. *Toxicol. Appl. Pharmacol.* **217**, 289-298.
Rubinsky, B., Lee, C. Y., Bastacky, J. and Onik, J. (1990). The process of freezing and the mechanism of damage during hepatic cryosurgery. *Cryobiology.* **27**, 85-97.
Schiller, T. M., Costanzo, J. P. and Lee, R. E. (2008). Urea production capacity in the wood frog (Rana sylvatica) varies with season and experimentally induced hyperuremia. *J. Exp. Zool. A. Ecol. Genet. Physiol.* **309**, 484-493.
Simpson, P. J. and Lucchesi, B. R. (1987). Myocardial ischemia: the potential therapeutic role of prostacyclin and its analogues. In *Prostacyclin and Its Stable Analogue Iloprost* (ed R. J. Gryglewski and G. Stock), pp. 179-194. Berlin Heidelberg: Springer.
Storey, K. B. (1990). Life in a frozen state: adaptive strategies for natural freeze tolerance in amphibians and reptiles. *Am. J. Physiol.* **258**, R559-R568.
Storey, K. B. and Storey, J. M. (1984). Biochemical adaption for freezing tolerance in the wood frog, *Rana sylvatica*. *J. Comp. Phys. B.* **155**, 29-36.
Storey, K. B. and Storey, J. M. (2004). Physiology, biochemistry and molecular biology of vertebrate freeze tolerance: the wood frog. In *Life in the Frozen State* (ed. E. Benson B. Fuller and N. Lane), pp. 243-274. Boca Raton: CRC Press.
Tesfamariam, B. and Cohen, R. A. (1992). Free radicals mediate endothelial cell dysfunction caused by elevated glucose. *Am. J. Physiol.* **263**, H321-H326.
Valko, M., Morris, H. and Cronin, M. T. (2005). Metals, toxicity and oxidative stress. *Curr. Med. Chem.* **12**, 1161-1208.
Willmore, W. G. and Storey, K. B. (1997). Antioxidant systems and anoxia tolerance in a freshwater turtle *Trachemys scripta elegans*. *Mol. Cell. Biochem.* **170**, 177-185.
Zweier, J. L. and Talukder, M. A. H. (2006). The role of oxidants and free radicals in reperfusion injury. *Cardiovasc. Res.* **70**, 181-190.